

Competition on Nitrocellulose-Immobilized Antibody Arrays: From Bacterial  
Protein Binding Assay to Protein Profiling in Breast Cancer Cells

**Garabet Yeretssian<sup>1</sup>, Michèle Lecocq<sup>2</sup>, Guillaume Lebon<sup>2</sup>, Helen C Hurst<sup>3</sup> and Vehary  
Sakanyan<sup>1, 2</sup> \***

<sup>1</sup> Biotechnologie, Biocatalyse, Biorégulation, UMR CNRS 6204, Université de Nantes, 2 rue de  
la Houssinière, 44322 Nantes, France

<sup>2</sup> ProtNeteomix, Université de Nantes, 2 rue de la Houssinière, 44322 Nantes, France

<sup>3</sup> Cancer Research UK Molecular Oncology Unit, Barts' and The London School of Medicine,  
London EC1M 6BQ, UK

**Running title: Competition-based protein profiling on antibody arrays**

\* To whom correspondence should be addressed:

Vehary Sakanyan

Tel: (33) 251125620; Fax: (33) 251125637

E-mail: [Vehary.Sakanyan@chimbio.univ-nantes.fr](mailto:Vehary.Sakanyan@chimbio.univ-nantes.fr)

[v.sakanyan@protneteomix.com](mailto:v.sakanyan@protneteomix.com)

## ABBREVIATIONS

Ab, antibody

AIDS, Acquired Immune Deficiency Syndrome

ANOVA, Analysis Of Variance

AP-2, Activator Protein-2

BSA, Bovine Serum Albumin

Cdk, Cyclin dependent kinase

ERK1, Extracellular signal regulated kinase 1

FBS, Foetal Bovine Serum

IgG, immunoglobulin G

IPTG, isopropyl-1- $\beta$ -D-thio-1-galactopyranoside

IRDye, near-infrared fluorescence dye

JNK1/2, c-Jun N-terminal kinase 1/2

LB medium, Luria-Bertani medium

mAb, monoclonal antibody

MDM2, Mouse double minute 2 protein

NC, nitrocellulose

NHS, N-hydroxysuccinimide

Ni-NTA, Nickel - Nitrilotriacetic Acid

NMRAT, Normalized ratio

OD<sub>600</sub>, optical density at 600 nm

pAb, polyclonal antibody

PBS, Phosphate Buffered Saline

PBS-T, Phosphate Buffered Saline with Tween 20

Rb, Retinoblastoma

RNAP, RNA polymerase

SDS - PAGE, Sodium Dodecyl Sulfate - Polyacrylamide Gel Electrophoresis

VEGF, Vascular Endothelial Growth Factor

## **KEYWORDS**

Antibody array, competitive displacement, protein profiling, breast cancer, RNA polymerase, near-infrared fluorescence.

## **SUMMARY**

Large-scale comparative evaluation of protein expression requires miniaturized techniques to provide sensitive and accurate measurements of the abundance of molecules present as individual and/or assembled protein complexes in cells. The principle of competition between target molecules for binding to arrayed antibodies has recently been proposed to assess differential expression of numerous proteins with one-color or two-color fluorescence detection methods. To establish the limiting factors, and to validate the use of alternative detection for protein profiling, we performed competitive binding assays under different conditions. A model experimental protocol was developed whereby the competitive displacement of multi-subunit bacterial RNA polymerase and/or its subunits was evaluated through binding to subunit-specific immobilized monoclonal antibodies. We show that the difference in physico-chemical properties of unlabeled and labeled molecules significantly affects the performance of one-color detection, whereas epitope inaccessibility in the protein complex can prohibit the assessment of competition by both detection methods. Our data also demonstrate that antibody cross-reactivity, target protein truncation and abundance, as well as the cellular compartment of origin are major factors that affect protein profiling on antibody arrays. The experimental conditions established for prokaryotic proteins were adopted to compare protein profiles in the breast tumor-derived cell lines, MDA MB-231 and SKBR3. Competitive displacement was detected and confirmed for a number of proteins using both detection methods; however, we show that overall the two-color method is better suited for accurate expression profile evaluation of a large, complex set of

proteins. Antibody array data confirm the functional linkage between the ErbB2 receptor and AP-2 transcription factors in these cell lines and highlight unexpected differences in G<sub>1</sub> cyclin expression.

## INTRODUCTION

One of the great challenges in the field of post-genomic research is the large-scale evaluation of protein expression in a variety of human pathologies, using miniaturized techniques to provide high sensitivity, short assay times and minimal reagent consumption. Protein spots arranged in macroarray or microarray formats on planar supports are an attractive technique to use in this context, with the potential for high-throughput dissection of molecular interactions and the possibility of diversifying the array format to study a huge number of defined and/or non-characterized proteins (1).

Many diseases are associated with, or even result from, modulations in protein expression. Therefore, monitoring simultaneously the expression profiles of a large number of proteins by antibody arrays can provide important information about the physiological status of the organism and can help to identify disease-specific biomarker candidates (2). Two main strategies have been proposed to compare and evaluate protein expression in cell lysates, both based on protein competition for binding to arrayed antibodies. The two-color approach detects differences in protein concentration between two cell lysates labeled by different fluorescent dyes and mixed in an equal ratio (3; 4). Two parallel experiments are run with mutually exchanged fluorescent dyes to reduce the possible interference from bio-conjugation bias of the dyes to proteins in the two samples. This method has been applied to evaluate protein profiling in human cancer cells and tissues (5; 6; 7; 8; 9; 10; 11; 12; 13). Recently a one-color approach

(referred to as “competitive displacement”) has been described which detects protein variations in lysates when the reference sample alone is labelled with a fluorescent dye (14; 15). Fluorescence intensity decreases differentially to be equivalent to, greater or less than 50% displacement depending on the abundance of unlabeled proteins mixed in equal quantity with the labeled reference. This cost-effective approach appears to be more convenient for large-scale proteomic investigations. However, no data are available demonstrating the real competitiveness of labeled and unlabeled proteins on an antibody array and it is important, therefore, to assess displacement activity in a single protein competitive binding assay, and to compare directly the performance of these two protein profiling detection methods.

In cells many proteins are assembled into structural complexes in which a target epitope might be masked and thus not recognized by the corresponding antibody. To address this issue, we have used bacterial RNA polymerase (RNAP), a complex protein model assembled *via* the dimerization of  $\alpha$  subunits and the binding of  $\beta$ ,  $\beta'$ ,  $\omega$  and one of the exchangeable  $\sigma$  subunits into a functionally active holoenzyme recognizing specific promoter sequences (16). In order to evaluate the one-color and two-color detection methods in protein profiling with antibodies arrayed on a nitrocellulose (NC) membrane, we have chosen near-infrared fluorescent dyes (IRDyes) for labeling proteins. Near-infrared fluorescence provides high sensitivity on membrane supports (17) and has been successfully used to detect molecular interactions on arrayed purified proteins (18), phage displayed peptides (19), rat neuronal membrane fractions (20) and crude prokaryotic extracts (21). As the *Escherichia coli*  $\alpha$  subunit of RNAP ( $\alpha$ RNAP),

labeled by IRDye, retains its binding ability to arrayed transcriptional factors (21), it has been used as a reporter to assess the competitiveness of labeled and unlabeled molecules in binding assays.

The information acquired from competition between individual prokaryotic proteins (RNAP and its subunits) has been used to compare more complex protein expression profiles in breast tumor-derived MDA MB-231 and SKBR3 cell lines with the aim of gaining insight into the functional grouping of targets involved in regulatory pathways. The data obtained with both detection methods were concordant for a few proteins; however, two-color detection allowed the abundance of a greater number of target proteins to be assessed and we therefore conclude that this technique is better suited to high-throughput protein profiling.

## EXPERIMENTAL PROCEDURES

*Affinity purification of tagged proteins* The plasmid pET rpoA-his carrying the *E. coli* gene *rpoA* coding for  $\alpha$ RNAP with a C-terminal His-tag has been described previously (21). The recombinant protein was purified from *E. coli* BL21Star (DE3) (pET\_rpoA-his) cells grown in Luria-Bertani (LB) medium after induction with 1 mM isopropyl-1- $\beta$ -D-thio-1-galactopyranoside (IPTG) at 37°C for 5 h on a nickel-nitrilotriacetic acid (Ni-NTA) column according to the manufacturer's recommendations (Qiagen, CourtaBœuf, France). To express simultaneously the *E. coli* RNA polymerase  $\alpha$ ,  $\beta$ ,  $\beta'$  and  $\omega$  subunits, and to purify the whole protein complex, we used a duet expression system composed of two compatible pET duet1 and pACYC duet1 vectors (Novagen, Fontenay-sous-bois, France) carrying respectively cloned his-rpoA, rpoB and rpoC, rpoZ genes. Details of the construction of pET duet1 his-rpoA, rpoB / pACYC duet1 rpoC, rpoZ and the purification of RNAP will be presented elsewhere (Lebon G., Marc F., Sakanyan V. *in preparation*). The purified RNAP was compared with a commercial preparation (Epicentre, Madison, Wisconsin): protein purity was ascertained on a 12% SDS-PAGE followed by densitometry analysis.

*Preparation of bacterial lysates for competition experiments* – Recombinant *E. coli* BL21 Star (DE3) strain (Invitrogen, Cergy Pontoise, France), carrying the plasmids pET rpoA-his or

pET duet1 his-rpoA, rpoB / pACYC duet1 rpoC, rpoZ, were grown in LB medium to an OD<sub>600</sub> of 0.6-0.8 and induced with 1 mM IPTG for up to 5 h. Aliquots were taken at 0, 1, 2 and 5 h of incubation, harvested by centrifugation and resuspended in lysis buffer containing 50 mM NaH<sub>2</sub>PO<sub>4</sub> pH 8.0, 300 mM NaCl, 10 mM imidazole, 1 mg/mL lysozyme. The cells, after incubation at 4°C for 2 h, were sonicated and cleared by centrifugation. The supernatant was filtered through 0.2 µm hydrophilic sterile filters (Fisher Labosi, Elancourt, France). This step significantly reduced fluorescent "noise" during subsequent assays on NC-membrane immobilized antibody arrays. Total protein concentration was measured by a biophotometer (Eppendorf) using the bicinchoninic acid method (22) or the Bradford method (23) with BSA as the calibration standard. If necessary the lysates were labeled and used to assess competition of respective proteins under different experimental conditions (see Results).

*Preparation of eukaryotic lysates for competition experiments* – Human breast carcinoma cell lines MDA MB-231 and SKBR3 were grown in Dulbecco's Modified Eagle's Medium with 4.5 g/L glucose and L-glutamine (BioWhittaker, Belgium) containing 10% FBS (BioMedia, Boussens, France) and 11.2 U/L penicillin/11.2 µg/L streptomycin at 37°C and 5% CO<sub>2</sub>. Cells were washed 3 times with PBS (137 mM NaCl, 2.7 mM KCl, 4.3 mM Na<sub>2</sub>HPO<sub>4</sub> pH 7.4) and lysed in PBS with 1% NP-40 and 1x protease inhibitor mixture at 4°C for 15 minutes. Cellular DNA was sheared by brief sonication and the solubilized proteins were harvested by

centrifugation at 13000 rpm for 15 minutes. Subcellular Proteome Extraction kit (Calbiochem, Fontenay sous bois, France) was also used in order to recover a higher proportion of non-denatured target proteins from various cellular compartments. The yield and quality of partial proteomes corresponding to cytosolic, membrane/organelle, nucleus and cytoskeleton proteins were verified by SDS-PAGE analysis according to the manufacturer's recommendations. Protein concentration was determined as described above.

*Labeling purified and total proteins in cell lysates with IRDyes* – Purified proteins and prokaryotic or eukaryotic lysates were labeled with Alexa Fluor 680 (Molecular Probes, Cergy Pontoise, France) and/or IRDye 800CW (LiCOR Biosciences, Lincoln, NE, USA) using a protocol adopted from Molecular Probes. Briefly, 5  $\mu$ L of freshly prepared 1 M sodium bicarbonate buffer pH 8.3 was added to 50  $\mu$ L of 2 mg/mL protein solution with the corresponding fluorescent dye, then incubated in the dark for 1 h with gentle shaking. The conjugated dye-protein complex was separated from free dye by gel filtration and eluted with PBS buffer. The average number of conjugated dye molecules was estimated, and samples with a final molar ratio 2-3 dye molecules to 1 protein molecule were used to evaluate protein competitiveness in binding assays. Protein concentration was determined with a biophotometer as described above.

*Western blotting* – 10  $\mu$ g total protein of prokaryotic cell extracts or 40  $\mu$ g total protein of

eukaryotic cell extracts were separated on 12% SDS-PAGE and transferred to NC-membrane. After blocking with PBS/ 0.05% Tween 20 / 5% skimmed milk, the membrane was incubated with the corresponding monoclonal primary antibody in PBS / 0.05% Tween 20 / 3% BSA at room temperature for 2 h. After washing in PBS / 0.05% Tween 20, the membrane was incubated for 1 h with Alexa Fluor 680 goat anti-mouse IgG secondary antibody or IRDye 800 conjugated affinity purified goat anti-rabbit IgG (LI-COR, Lincoln, NE, USA). Fluorescent detection was achieved by scanning the membranes at 700 or 800 nm using the Odyssey Infrared Imaging system (LI-COR, Lincoln, NE, USA). The fluorescent protein bands were quantified by Molecular Analyst (BioRad Laboratories, Marne-La-Coquette, France).

*Preparation of antibody arrays* – Both monoclonal (mAb) and polyclonal antibodies (pAb) against selected proteins were used to fabricate several designs of arrays with different sets of antibodies depending on the experimental purpose. The mAbs generated against *E. coli* RNA polymerase subunits  $\alpha$  (mAb clone 4RA2),  $\beta$  (mAb clone NT63) and  $\beta$  (mAb clone NT73) were purchased from NeoClone Biotechnology International, USA. Antibodies against eukaryotic proteins involved in stress response, cell cycle progression, oncogenesis, apoptosis and metastases were purchased from Interchim (Montlucon, France), BD PharMingen (San Diego, CA), Sigma-Aldrich (Lyon, France) and VWR International (Fontenay sous Bois). AP-2 $\alpha$  (clone 8G8) and AP-2 $\gamma$  (clone 6E4) mAbs were described previously (24). Antibodies were serially two-fold titrated within a range of 1 to 0.125 mg/mL and printed on glass slides covered

in-house with Protran BA83 NC-sheet or on commercial FAST™ slides (Schleicher & Schuell, Equevilly, France) using a manual microarray system (Microcaster, Schleicher & Schuell, Equevilly, France).

*Binding assays* – Two methods were used to evaluate protein binding to NC-immobilized antibodies. To assess competitive displacement by one-color detection (14), the arrayed membranes were blocked prior to use in PBS containing 0.1-2% Tween 20 by slow agitation on a platform rocker at room temperature for 1 h. The blocking solution was discarded and membranes were then incubated with a labeled probe (usually at 1 µg/mL concentration) or with a mixture of labeled and unlabeled protein samples. If necessary, a competitive unlabeled sample (as purified protein or total protein in lysates) was added at increasing ratios corresponding to 1, 10 or 100 µg/mL of total protein concentration. Membranes were incubated at room temperature for 30 min, washed three times with high-salt PBS-T buffer (PBS containing 500 mM sodium chloride and 0.1% Tween 20) and then dried. Fluorescent signals were detected by scanning membranes with the Odyssey Infrared Imaging system (LI-COR, Lincoln, NE, USA).

In two-color detection, antibody arrays were incubated with an equal mixture of samples labeled with IRDye 800CW and Alexa Fluor 680 under the conditions described above, and washed using a Protein Array Workstation (Perkin Elmer, London, UK).

*Data acquisition and statistical analysis* – The software GenePix Pro 4.0 (Axon Instruments, Union City, CA, USA) was used to quantify the image data. The local background in the near-infrared fluorescent wavelength channel was subtracted from the fluorescent signal registered from each antibody spot. Only spots displaying a fluorescent intensity greater than twice the level of background noise were used for further analysis.

Mean values of quadruplicate readings were used for the analysis of fluorescent intensity from spots detected by the one-color method. The degree of competition between labeled and unlabeled samples displaced at a 1:1 ratio (the best statistical fit to monitor displacement), were subtracted from values obtained after competition between the same labeled reference and another unlabeled sample.

In the two-color evaluation, data were scaled such that the average mean ratio value for all of the spots on each separate array was normalized to 1, with the premise that the average spot on the chip would represent unchanged protein expression. A data-based criterion was determined, above or below which proteins were found to be differentially expressed. To determine such a cutoff level, a hierarchical model approach was used (4) in which the parameters were estimated using ANOVA.

Normalized ratio (NMRAT) values outside the interval of 0.72-1.28 were considered differentially expressed with 95% statistical confidence when analyzing *E. coli* cell extracts in imitation experiments. NMRAT values outside the interval of 0.83-1.17 and 0.73-1.27 were considered differentially expressed with respectively, 70% and 90% statistical confidence when

analyzing total protein lysates of breast cancer MDA MB-231 and SKBR3 cell lines. To analyze proteins derived from the nuclear sub-fraction of the same cell lines, NMRAT values outside the intervals 0.82-1.18 and 0.71-1.29 were considered differentially expressed with respectively, 70% and 90% statistical confidence.

## RESULTS

*Rationale of the protein competition assay on NC-immobilized antibody arrays* – A general schema of the protocol used to assess single-protein competition on antibody arrays is shown in Fig. 1B. Epitopes of the *E. coli* RNA polymerase  $\alpha$ ,  $\beta$  and  $\beta'$  subunits were used to follow the displacement of the purified  $\alpha$ RNAP protein or the whole RNAP protein complex or the overexpressed proteins in crude extracts obtained from IPTG-induced cells.

Barry and co-workers used hydrogel-arrayed antibodies to carry out competitive displacement of proteins followed by one-color detection (14). We were concerned that such a support might differentially affect the penetration of labelled and unlabeled samples into the gel, and therefore chose to print antibodies onto an NC-membrane, which we have previously shown to be highly efficient in studying molecular interactions using IRDye-labeled probes (21).

A four-parameter logistic regression method (25), used for competitive binding immunoassays, was applied to construct a plot of signal intensity versus analyte concentration.

Equation 1:

$$y = \frac{a-d}{1+(x/c)^b} + d$$

This shows the inverse relationship between the fluorescent signal  $y$  (fluorescence intensity at 700 nm or 800 nm) and the concentration of the unlabeled analyte  $x$  (protein in  $\mu\text{g/mL}$ ) in which  $a$ , is the maximum fluorescence estimated at zero concentration of  $x$ ;  $b$ , the slope factor for the

transition between **a** and **d**; **c**, the mid-range concentration of analyte corresponding to the point of inflection on the sigmoid and **d**, the minimal signal at infinite **x** concentration corresponding to the background detected on an NC-membrane. Signals can be normalized as a ratio of **B** and  $B_0$  corresponding to two fluorescent signals calculated respectively as **a - d** and **y - d**.

Assuming that no dissociation and rebinding occurs under the standardized conditions, the competition between labeled and unlabeled proteins for the single antibody epitope should lead to 50%, 90% and 99% displacement respectively at a mixed labelled : unlabeled sample ratio of 1:1, 1:10 and 1:100 as compared to the labelled reference protein or lysate. A typical competitive displacement curve for the purified bacterial  $\alpha$ RNAP, displayed on a semi-log plot, shows that the diminution of the fluorescent signal intensity (%  $B/B_0$ ) is dependent on an increase in the unlabeled analyte concentration within a detectable concentration range of immobilized antibodies (Fig. 2).  $B/B_0$  was plotted against the logarithm of the concentration of unlabeled  $\alpha$ RNAP using Origin 7.0 software (OriginLab Corporation, Northampton, USA).

*Competition between purified  $\alpha$ RNAP molecules* In preliminary experiments, Alexa Fluor 680-labeled  $\alpha$ RNAP, at concentrations ranging from 0.1 to 10  $\mu$ g/mL in the binding solution, was incubated with anti- $\alpha$ RNAP mAb printed from two-fold titrated antibody samples on a NC-membrane. Increasing fluorescent background was observed at concentrations above 1  $\mu$ g/mL, therefore, further measurements were performed at this concentration for all labeled

analytes tested.

Next, the immobilized anti- $\alpha$ RNAP mAb (printed from two-fold titrated solutions at concentrations ranging from 1 to 0.06 mg/mL) was probed with labeled  $\alpha$ RNAP alone or a mixture of labeled : unlabeled  $\alpha$ RNAP at various ratios. A diminution in the fluorescent signal, close to the expected theoretical values, was detected from spots corresponding to anti- $\alpha$ RNAP from 1 and 0.5 mg/mL antibody dilutions (see Fig. 2). The signal was weaker and poorly interpretable from spots printed at antibody concentrations less than 0.25 mg/mL. Therefore, further measurements were done by taking into account only signal intensities detected on spots printed from 1 and 0.5 mg/mL antibody concentrations.

To evaluate the accuracy of the competition between  $\alpha$ RNAP molecules, we took advantage of the two-color fluorescent detection method, enabling us to monitor the behavior of identical molecules labeled differentially. Purified  $\alpha$ RNAP samples, separately labeled with Alexa Fluor 680 and IRDye 800CW, were mixed in different ratios and probed with the immobilized anti- $\alpha$ RNAP mAb. The reduction in fluorescent intensity at 700 nm (Fig. 3A) was accompanied by the appearance of a fluorescent signal at 800 nm (Fig. 3B). A good correlation in the modulation of the signal intensity confirmed the inverse relationship of the binding competition between two identical proteins, for the anti- $\alpha$ RNAP monoclonal antibody arrayed on an NC-membrane (Fig. 3C).

*Competitive displacement of  $\alpha$ RNAP in bacterial cell lysates* To assess the

competitiveness of  $\alpha$ RNAP in more complex bacterial cell extracts, we determined the displacement of this protein synthesized in *E. coli* BL21Star (DE3) (pET rpoA-his) cells, obtained after 1 h IPTG induction of the *rpoA* gene, using labeled sample mixed with the purified unlabeled protein. A strong, 75% diminution of the signal was detected after addition of an equal amount purified  $\alpha$ RNAP (data not shown) indicating that the concentration of the target protein was lower in the crude lysates than the concentration of the added protein. In contrast, when a mixture of labeled and unlabeled lysates of *E. coli* BL21Star (DE3) (pET rpoA-his) of 1 h induced cells was tested, the displacement was more reminiscent of that observed between purified  $\alpha$ RNAP molecules (see Fig. 2).

*Competition between  $\alpha$ RNAP and the RNAP complex* Next, we were interested in determining whether competition occurs between small  $\alpha$ RNAP and large RNAP molecules. A labeled lysate (1  $\mu$ g/mL total protein), of the *E. coli* BL21Star (DE3) (pET rpoA-his) cells, induced with IPTG for 1 h, was competed with purified unlabeled RNAP. A clear diminution in fluorescence intensity was detected corresponding to 30% and 70% displacement of  $\alpha$ RNAP, respectively for 1:1 and 1:10 ratios (Fig. 4A). However, this displacement rate was weaker compared to the competition between individual  $\alpha$ RNAP molecules (see the previous section).

To confirm the competitiveness of whole RNAP, we also tested lysate of *E. coli* BL21Star (DE3) (pET duet1 his-rpoA, rpoB / pACYC duet1 rpoC, rpoZ) cells, induced with IPTG for 1 h to allow simultaneous overexpression and assembly of  $\alpha$ ,  $\beta$ ,  $\beta'$  and  $\omega$  subunits into a whole RNAP enzyme. Competition between the labeled lysate and the unlabeled purified

$\alpha$ RNAP resulted in strong 85 % and 95% displacement, respectively at 1:1 and 1:10 ratios (Fig. 4B).

These data showed that  $\alpha$ RNAP and the RNAP complex can compete for immobilized anti- $\alpha$ RNAP monoclonal antibody. However, the large protein complex was less competitive compared to the smaller  $\alpha$ RNAP molecule and this can be explained, at least partially, by the lower molar presentation of the  $\alpha$ -subunit in RNA polymerase.

*Competitive displacement of the RNAP complex in bacterial cell lysates* – In order to gain insight into the competition behavior of a whole RNAP, we assessed its displacement in a mixture of labeled extract of *E. coli* BL21Star (DE3) (pET duet1 his-rpoA, rpoB / pACYC duet1 rpoC, rpoZ) cells after 1 h IPTG induction, and the unlabeled RNAP. The binding was followed in parallel assays with anti- $\alpha$ RNAP, anti- $\beta$ RNAP and anti- $\beta$ RNAP mAbs immobilized on the same NC-membrane. As shown in Fig. 4C, 55% and 95% displacement of the labeled lysate by unlabeled RNAP was detected with the anti- $\alpha$ RNAP mAb, respectively at 1:1 and 1:10 ratios. Low fluorescence was observed from anti- $\beta$ RNAP and anti- $\beta$ RNAP mAb spots, with and without addition of unlabeled RNAP, that indicated that no displacement occurred under the conditions used (data not shown).

Similar experiments were performed with labeled and unlabeled lysates from *E. coli* BL21Star (DE3) (pET duet1 his-rpoA, rpoB / pACYC duet1 rpoC, rpoZ) obtained from 1 h IPTG-induced cells. Again, displacement was clearly observed with the anti- $\alpha$ RNAP mAb, whereas no competition was detected with anti- $\beta$ RNAP and anti- $\beta$ RNAP mAbs (data not shown).

To clarify this discrepancy in the competitive displacement, we followed the kinetics of  $\alpha$ ,  $\beta$  and  $\beta$  subunit expression (as soluble proteins in the supernatant) in IPTG-induced cells of *E. coli* BL21Star (DE3) (pET duet1 his-rpoA, rpoB / pACYC duet1 rpoC, rpoZ) using Western blotting. As shown in Fig. 5, an abundant band corresponding to each protein appeared after 1h induction. Densitometry of these protein bands revealed that the yield of  $\alpha$ ,  $\beta$  and  $\beta$  subunits was respectively 11-, 6- and 4- fold greater in 1 h induced cells compared to non-induced ones. However, further induction of the cells up to 5 h resulted only in 1.3- and 1.8-fold further increases in the yield of  $\alpha$ RNAP and  $\beta$ RNAP, whereas the yield of  $\beta$ RNAP increased 1.6-fold after 2 h induction and thereafter decreased to the level of a 1 h induction.

Based on these data, we attempted to evaluate the competition between labeled lysates of 2 or 5 h induced cells and the unlabeled RNAP. Again, the displacement was only detected from spots with immobilized anti- $\alpha$ RNAP mAb but not with anti- $\beta$ RNAP and anti- $\beta$ RNAPmAbs (data not shown).

*Imitation of protein profiling using crude bacterial lysates* We next asked whether the competitive displacement can be detected in lysates obtained from bacterial host cells in which whole polymerase or its  $\alpha$  subunit were differentially expressed. To compare the amount of  $\alpha$ RNAP synthesized in 1 h and 2 h induced cells, we mixed labeled and unlabeled lysates at 1:1 ratio, and incubated the mixture with the arrayed anti- $\alpha$ RNAP mAb. The difference in protein expression deduced from the spots was found to be +25 % when the labeled reference was the 1

h induced lysate (Fig. 6A, compare the first two columns), whereas it was -15 % when the labeled reference was a 2 h induced lysate (Fig. 6A, compare the last two columns). Similar displacement values were obtained by following the behavior of RNAP in 1 h and 2 h induced cells, again using anti- $\alpha$ RNAP mAb for detection. However, no differential expression of RNAP was observed in cells when  $\beta$ RNAP / anti- $\beta$ RNAP mAb or  $\beta$ RNAP / anti- $\beta$ RNAP mAb couples were used for detection. The failure to detect the RNAP displacement with anti- $\beta$ RNAPmAbs was not related to small differences in the amount of 1 h and 2 h induced lysates (see Fig. 5), since negative results were also obtained with mixtures of 1 h and 5 h induced cell lysates (data not shown).

In order to find out whether profiling of RNAP can be detected on anti- $\beta$ RNAP or anti- $\beta$ RNAP arrayed mAbs by the alternative two-color fluorescence method, we mixed lysates from *E. coli* BL21Star (DE3) (pET duet1 his-rpoA, rpoB / pACYC duet1 rpoC, rpoZ) cells induced for 1 h or 5 h and labeled respectively, with Alexa Fluor 680 and IRDye 800CW. As shown in Fig. 6B, greater RNAP expression was detected in 5 h induced cells *versus* 1 h induced cells following anti- $\beta$ RNAP mAb (NMRAT of 1.54) and anti- $\alpha$ RNAP mAb (NMRAT of 1.30) with 95% statistical confidence, whereas no difference was observed with the anti- $\beta$ RNAP mAb as it had an NMRAT value of 0.93, that is in the range of 0.72-1.28 (see Experimental Procedures).

*Comparative protein profiling in breast cancer cells by one-color and two-color detection* Given the data obtained with “profiling” bacterial RNAP, we used one-color and

two-color methods to evaluate their performance in assessing the differential expression of numerous proteins in breast cancer cell lines. An array of 72 selected antibodies was prepared by spotting each antibody in quadruplicate on FAST slides.

First, we compared the competitive displacement of labeled total proteins from MDA MB-231 cell lysates by unlabeled proteins from the same lysate. A decrease in fluorescence intensity was observed for many spots when mixing the two lysates at 1:1 and 1:10 ratios, as compared to the reference array bound labeled lysate alone (Fig. 7, slides 1 and 2 and data not shown). We used data from the most informative 28 antibodies that gave the highest signals, and analyzed the displacement characteristics at two ratios of mixed lysates. The expected theoretical values of ~50% and ~90% fluorescence diminution were detected for only 10 and 8 spots respectively, whereas other spots gave significant deviations from the expected displacement values.

Next, we mixed labeled lysate from MDA MB-231 cells with unlabeled lysate from SKBR3 cells at 1:1 and 1:10 ratios, and evaluated the competitive displacement between proteins from the two cell lines (Fig. 7 and data not shown). The difference in fluorescence intensity displayed as MDA MB-231 displacement minus SKBR3 displacement, showed increased abundance of AP-2 $\alpha$ , VEGF, p53, ErbB2, catalase, MDM2, thymidylate synthase and ERK1 proteins in SKBR3 cells.

In a parallel assay with the same antibody array, total proteins from the MDA MB-231 and SKBR3 cell lines were analyzed by two-color fluorescence detection (Fig. 8). Seven

proteins, AP-2 $\alpha$ , cyclin D<sub>3</sub>, cyclin E, thymidylate synthase, catalase, 14.3.3 sigma and ErbB2, were found to be more abundant in SKBR3 cells than in MDA MB-231 cells with 70% statistical confidence. Moreover, even at the more stringent 90% statistical confidence level, 14.3.3 sigma and ErbB2 were still found to be up-regulated in SKBR3 cells.

Higher abundance was confirmed for 5 proteins, AP-2 $\alpha$ , cyclin E, catalase, 14.3.3 sigma and ErbB2, in SKBR3 cells by western blot analysis (see Fig. 8). In contradiction of the one-color results, weaker bands were detected for MDM2 (data not shown) and p53 proteins in SKBR3 cells compared to MDA MB-231, in agreement with previous data (26). We did not detect bound bands for cyclin D<sub>3</sub> or thymidylate synthase, which may be explained either by too low abundance to be detected by western blot or by their degradation during storage. Two control proteins, ERK1 and  $\beta$ -actin, which are known to be synthesized at equal levels in the both cell lines (27; 28), showed bands of almost identical intensity in the corresponding lysates.

These data indicated that both the one-color and two-color methods detected differential expression of the same 4 proteins, AP-2 $\alpha$ , catalase, thymidylate synthase and ErbB2. However, overall two-color detection was more reliable than the one-color method in terms of its capacity to evaluate precise differential expression of a greater number of proteins in cells under the conditions used.

*Improving protein profiling with enriched nuclear proteins using the two-color method –*

Analysis of NMRAT values indicated that some nuclear proteins showed a tendency towards differential expression with 60% statistical confidence when total protein lysates were used for profiling with the two-color method. Assuming that nuclear proteins are under represented in our total cellular lysates, we wondered whether the profiling performance could be improved using an enriched nuclear sub-fraction.

We therefore performed similar experiments with nuclear extracts from MDA MB-231 and SKBR3 cell lines, followed by two-color fluorescence detection. Eight proteins were found to be differentially expressed. Cyclin D<sub>1</sub>, AP-2 $\alpha$ , AP-2 $\gamma$ , cyclin E and cyclin D<sub>3</sub> were expressed at higher levels in SKBR3 cells, whereas, p53, c-Jun and JNK1/2 were reduced in the same cells with 70% statistical confidence (Fig.9). The remarkable differential expression of AP-2 $\alpha$ , cyclin E, cyclin D<sub>3</sub>, AP-2 $\gamma$  and JNK1/2 was further validated using a more stringent NMRAT interval of 0.71-1.29 corresponding to 90% statistical confidence. Western blotting of total protein from MDA MB-231 and SKBR3 cells confirmed that cyclin D<sub>1</sub> and AP-2 $\gamma$  were overexpressed in SKBR3 cells, whereas c-Jun and JNK1/2 were at a lower abundance in these cells (see Fig. 8). The presence of two bands for JNK1/2 is due to recognition of the same epitope on two related JNK proteins by the anti-JNK1/2 mAb. These data confirmed that nuclear protein sub-fractionation provides more precise profiling information about the nuclear proteome in these cells.

## DISCUSSION

High-throughput protein profiling allows the measurement of the relative concentration of numerous target molecules in two analytes using a single binding assay with immobilized antibodies. Two different evaluations based on the competition principle, termed one-color and two-color detection, have been proposed to study protein profiling in human cells and tissues. Considering the potential advantages of one-color detection (14), we have performed a detailed competitive displacement study of selected target proteins, presented as single- or multi-subunit complex molecules, to evaluate fully the strengths and weaknesses of this method.

A model protocol, composed of monoclonal antibodies immobilized on an NC-membrane probed with bacterial RNA polymerase subunits and analytes containing purified or non-purified target proteins, showed that one-color detection provides an accurate assessment of the competitiveness of  $\alpha$ RNAP or RNAP, when displacement is determined with an anti- $\alpha$ RNAP mAb. In contrast, no displacement of RNAP could be detected using anti- $\beta'$ RNAP mAbs with the one-color method whereas this was possible with the same mAb using the two-color evaluation. How can this discrepancy be explained?

Random conjugation of almost 1 kDa of fluorescent dyes to the reference protein (2-3 dye molecules/protein) increases, not only a protein's molecular mass, but also affects its folding, solubility, migration and molecular recognition properties. As a consequence, the competitiveness of labeled proteins can be dramatically changed with respect to unlabeled ones

when evaluated by one-color detection. In contrast, in two-color evaluation, both protein samples are labeled by chemically similar dyes through amine reactive NHS ester bonds of the IRDyes. Even if physico-chemical properties are disrupted in the labeled proteins, the two samples remain highly similar to each other and hence are likely to display similar competition activity for the antibody, and thus the displacement better reflects protein expression differences in mixed analytes. Moreover, running two binding assays in parallel with mutually exchanged dyes results in, after normalization, a significant decrease in interference from dye conjugation bias.

These conclusions were born out when we profiled complex protein mixtures in breast cancer cell lysates using the two detection methods. The expression profile determined for several proteins using the one-color method was not confirmed by western blot. However, the two-color method detected modulations in the level of expression of proteins that were not revealed using one-color detection. Therefore, we conclude that two-color profiling extends the utility of fluorescent assessment to a larger number of target proteins and is clearly better suited to high-throughput analysis of differential expression of complex proteomes from mammalian cells.

The specificity of antigen-antibody interaction is a function of their mutual affinity and antibody cross-reactivity and this takes on a special significance in protein profiling studies (29; 30; 31). Indeed, we have found that data obtained from some spots is impossible to interpret because of the high cross-reactivity of the antibodies as revealed by subsequent western blot

analysis. In addition, this study raises other important issues that can be useful for further improving the performance of high-throughput protein profiling with array technology.

Western blot analysis has shown that anti- $\beta$ RNAP and anti- $\beta$ 'RNAP mAbs bind to many smaller molecular weight species that accumulated in lysates from IPTG-induced cells (see Fig. 5). Such a pool of truncated  $\beta$  and  $\beta$ ' subunits can interfere with the competitive displacement of whole RNAP assembled from full-length subunits. Notably, truncated derivatives were also observed for overexpressed cyclin E, 14.3.3 sigma and ErbB2 in SKBR3, as well as for c-Jun in MDA MB-231 breast cancer cells. Therefore, we suggest that the presence of truncated proteins will contribute to a diminution in the specificity of antigen-antibody interactions and can thereby disrupt protein profiling performance.

We have also shown that the assessment of RNA polymerase expression depends strongly on the accessibility of the target epitopes by anti-subunit monoclonal antibodies. Neither of the two methods detected variations in RNAP expression when competition was monitored by  $\beta$  subunit binding to the anti- $\beta$ RNAP mAb. In agreement with this observation, the affinity purification of *E. coli* RNA polymerase using anti- $\beta$ RNAP mAb has been found to be inefficient in comparison with anti- $\alpha$ RNAP and anti- $\beta$ 'RNAP mAbs (32; 33). The 3D structure of the related *Thermus thermophilus* RNA polymerase is available (34) and suggests a logical explanation for these negative results. It turns out that the  $\beta$  epitope is almost completely masked by the other subunits, whereas the epitopes in the two  $\alpha$  and  $\beta$ ' subunits are exposed on the surface of the RNAP holoenzyme (see Fig. 1A). As many proteins are organized into multi-

molecular complexes in eukaryotic cells, we speculate that the efficiency of profiling proteins in their native state will be heavily influenced by the usually unpredictable accessibility of antibody recognition sites.

Low protein abundance is another limiting factor for protein profiling on minute planar spot surfaces when a total protein lysate is used. Near-infrared fluorescence allows the detection of attomol quantities of target molecules without signal amplification from protein patterns immobilized on a porous nitrocellulose support (21), with a sensitivity that is comparable to tyramide amplification and sufficient to assess the phosphorylation state in arrayed total proteins extracted from cancer biopsies (35). Unfortunately, the low proportion of target molecules in total protein lysates, used as solution analyte or as a printed analyte, strongly restricts the number of molecules that can be captured by the antibodies and thence be detected by near-infrared fluorescence. This limitation cannot be overridden by increasing the analyte concentration due to spot saturation. However, an analyte, enriched by target proteins isolated from the nucleus, can allow the identification of differential nuclear expression patterns which would not be detected using a total lysate. It appears that the use of a compartment-specific fraction provides both an augmentation in the proportion of target molecules in the analyte and a diminution in antibody cross-reactivity towards non-target molecules located in other cellular compartments. Both aspects are crucial to increase the specificity of antigen recognition and the sensitivity of protein profiling.

A major advantage of antibody array technology is the protein profiling of tumors in a

single experiment. Here, twelve proteins have been identified as increased or decreased in expression in two breast cancer cell lines, SKBR3 *versus* MDA MB-231, using a microarray prepared from 72 selected antibodies. Similar data obtained by other methods confirm these results for AP-2 $\alpha$  and AP-2 $\gamma$  (36), ErbB2 (37; 38), p53 (26) and c-Jun (37). A clear modulation of seven more proteins including three cyclins D<sub>1</sub>, D<sub>3</sub> and E, JNK1/2, thymidylate synthase, catalase and 14.3.3 sigma, underlies a wider pleiotropic effect of the cancer mutation(s) in the two cell lines.

The correlation between high levels of the AP-2 $\alpha$  and AP-2 $\gamma$  DNA binding transcription factors with overexpression of the *ERBB2* proto-oncogene in tumor-derived cell lines has been documented previously (36). The antibody array data presented here were able to confirm this functional linkage by detecting the up-regulation of the AP-2 factors in ErbB2 positive SKBR3 cells *versus* ErbB2 negative MDA MB-231 cells, particularly when protein lysates enriched for nuclear factors were employed (see Fig. 9). This provides an important validation of our methodology and supports the possibility of being able to derive biological information by comparing the proteomes of other tumor-derived cell lines and ultimately tumor samples and this is now under investigation.

We have also used our current data to compare more narrowly the biology of the two cell lines used in this study. Although not phenotypically alike, the two breast tumor-derived cell lines compared in this study share several features characteristic of poor prognosis breast cancer

patients. Both lines are negative for the estrogen receptor and also carry mutations in their p53 genes. Moreover, the MDA MB-231 line is noted for carrying an activated *Ha-Ras* gene and SKBR3 cells are extensively studied due to the amplification of their *ERBB2(neu)* gene which contributes to the overexpression of this receptor, as noted above (see Fig. 8). In breast epithelial cells, ErbB2 lies upstream of Ras in the mitogenic signaling pathway (39) which leads to transcriptional induction of cyclin D<sub>1</sub> (40; 41). Furthermore, activation of cyclin D<sub>1</sub> by this pathway is essential in this cell type as demonstrated by studies in cyclin D<sub>1</sub> null mice which are resistant to mammary carcinogenesis induced by either *ras* or *neu* oncogenes (42). By complexing with their partner kinases Cdk4/6 and Cdk2 to induce progressive phosphorylation and inactivation of pRb, the D-type and E-type cyclins control G<sub>1</sub> to S phase transition during normal cell cycle progression. Therefore, as both MDA MB-231 and SKBR3 cells are activated in essentially the same pathway and both have an intact *RB* gene, the levels of expression of these key growth factor target genes might be expected to be similar in the two cell lines. In our proteomic study however we find clear increased levels of cyclins D<sub>1</sub>, D<sub>3</sub> and E in SKBR3 cells compared to the MDA MB-231 line, particularly when nuclear extracts are compared (see Fig. 9). Previous comparison of these lines at the RNA level had not indicated these differences in expression level (43). This suggests therefore that for mitogenic cyclins, post-transcriptional regulation of their protein levels is important.

Given the apparently mammary-specific wiring of the *ERBB2/neu-Ras-cyclin D<sub>1</sub>*

pathway, it has been argued that an anti-cyclin D<sub>1</sub> therapy would be optimal for patients overexpressing ErbB2 (42). However, elevated cyclin E (both full length and low molecular weight forms) has also been associated with poor survival in this disease and in multivariate analysis was more closely associated with outcome than levels of cyclin D<sub>1</sub>, D<sub>3</sub> or ErbB2 (44). Moreover, since cyclin E acts downstream of cyclin D<sub>1</sub>, cells and tumors expressing even slightly elevated levels may bypass therapies targeted to cyclin D<sub>1</sub> alone. The subtle differences, highlighted here, between two lines activated in the same signaling pathway could therefore prove to be a useful model system to test the efficacy of such therapies.

The data presented here show that NC-prepared microarrays provide repetitive and precise measurements of antigen-antibody interactions through protein competition for corresponding antibodies using both eukaryotic and prokaryotic lysates. We have recently demonstrated the possibility of an accurate comparative assessment of the antibody binding affinity of IgG purified from the sera of AIDS patients using a panel of arrayed phage-displayed peptides (19). Together, these data are encouraging in terms of the development of reliable immunoassays to assess binding parameters of complex protein mixtures within a range of the sensitivity useful for biomedical investigations and applications.

## **ACKNOWLEDGEMENTS**

This study was supported by the “Post-Génome” program (Contrat Etat Région des Pays de la Loire). We greatly acknowledge Dr. Gabriel Ricolleau for discussions. G. Y. and G. L. are postgraduate students supported respectively by the National Council for Scientific Research Lebanon (CNRSL) and Ministère de la Recherche (ANRT) / ProtNeteomix.

## REFERENCES

1. Ekins, R., and Chu, F. In: J. S. Albala, I. Humphery-Smith (Eds.), Protein arrays, biochips, and Proteomics. The next phase of genomic discovery. Marcel Dekker, Inc. 2003, p. 81-125
2. Kodadek, T. (2001) Protein microarrays: prospects and problems. *Chem. Biol.* **8**, 105-115
3. Sreekumar, A., Nyati, M. K., Varambally, S., Barrette, T. R., Ghosh, D., Lawrence, T. S. and Chinnaiyan, A. M. (2001) Profiling of cancer cells using protein microarrays: discovery of novel radiation-regulated proteins. *Cancer Res.* **61**, 7585-7593
4. Haab, B. B., Dunham, M. J. and Brown, P. O. (2001) Protein microarrays for highly parallel detection and quantitation of specific proteins and antibodies in complex solutions. *Genome Biol.* **2**, RESEARCH0004

5. Knezevic, V., Leethanakul, C., Bichsel, V. E., Worth, J. M., Prabhu, V. V., Gutkind, J. S., Liotta, L. A., Munson, P. J., Petricoin, E. F., 3rd and Krizman, D. B. (2001) Proteomic profiling of the cancer microenvironment by antibody arrays. *Proteomics* **1**, 1271-1278
6. Huang, R. P., Huang, R., Fan, Y. and Lin, Y. (2001) Simultaneous detection of multiple cytokines from conditioned media and patient's sera by an antibody-based protein array system. *Anal. Biochem.* **294**, 55-62
7. Moody, M. D., Van Arsdell, S. W., Murphy, K. P., Orencole, S. F. and Burns, C. (2001) Array-based ELISAs for high-throughput analysis of human cytokines. *Biotechniques* **31**, 186-190, 192-194
8. Schweitzer, B., Roberts, S., Grimwade, B., Shao, W., Wang, M., Fu, Q., Shu, Q., Laroche, I., Zhou, Z., Tchernev, V. T., Christiansen, J., Velleca, M. and Kingsmore, S. F. (2002) Multiplexed protein profiling on microarrays by rolling-circle amplification. *Nat. Biotechnol.* **20**, 359-365
9. Tam, S. W., Wiese, R., Lee, S., Gilmore, J. and Kumble, K. D. (2002) Simultaneous analysis of eight human Th1/Th2 cytokines using microarrays. *J. Immunol. Methods* **261**,

157-165

10. Tannapfel, A., Anhalt, K., Hausermann, P., Sommerer, F., Benicke, M., Uhlmann, D., Witzigmann, H., Hauss, J. and Wittekind, C. (2003) Identification of novel proteins associated with hepatocellular carcinomas using protein microarrays. *J. Pathol.* **201**, 238-249
  
11. Miller, J. C., Zhou, H., Kwekel, J., Cavallo, R., Burke, J., Butler, E. B., Teh, B. S. and Haab, B. B. (2003) Antibody microarray profiling of human prostate cancer sera: antibody screening and identification of potential biomarkers. *Proteomics* **3**, 56-63
  
12. Nielsen, U. B., Cardone, M. H., Sinskey, A. J., MacBeath, G. and Sorger, P. K. (2003) Profiling receptor tyrosine kinase activation by using Ab microarrays. *Proc Natl. Acad. Sci. U.S.A.* **100**, 9330-9335
  
13. Zhou, H., Bouwman, K., Schotanus, M., Verweij, C., Marrero, J. A., Dillon, D., Costa, J., Lizardi, P. and Haab, B. B. (2004) Two-color, rolling-circle amplification on antibody microarrays for sensitive, multiplexed serum-protein measurements. *Genome Biol.* **5**, R28

14. Barry, R., Diggle, T., Terrett, J. and Soloviev, M. (2003) Competitive assay formats for high-throughput affinity arrays. *J. Biomol. Screen.* **8**, 257-263
15. Barry, R. & Soloviev, M. (2004) Quantitative protein profiling using antibody arrays. *Proteomics* **4**
16. Kimura, M. and Ishihama, A. (1996) Subunit assembly in vivo of Escherichia coli RNA polymerase: role of the amino-terminal assembly domain of alpha subunit. *Genes Cells* **1**, 517-528
17. Schutz, A. R., Altschuler, Y., Mostov, K. E., and Olive, D. M. (2000). Highly sensitive detection of proteins on membranes with near-infrared fluorescence. On-line posters, [www.licor.com](http://www.licor.com).
18. Ghochikyan, A., Karaivanova, I. M., Lecocq, M., Vusio, P., Arnaud, M. C., Snapyan, M., Weigel, P., Guevel, L., Buckle, M. and Sakanyan, V. (2002) Arginine operator binding by heterologous and chimeric ArgR repressors from Escherichia coli and Bacillus stearothermophilus. *J. Bacteriol.* **184**, 6602-6614
19. Arnaud, M. C., Gazarian, T., Rodriguez, Y. P., Gazarian, K. and Sakanyan, V. (2004)

- Array assessment of phage-displayed peptide mimics of Human Immunodeficiency Virus type 1 gp41 immunodominant epitope: binding to antibodies of infected individuals. *Proteomics* **4**, 1959-1964
20. Saghatelian, A. K., Snapyan, M., Gorissen, S., Meigel, I., Mosbacher, J., Kaupmann, K., Bettler, B., Kornilov, A. V., Nifantiev, N. E., Sakanyan, V., Schachner, M. and Dityatev, A. (2003) Recognition molecule associated carbohydrate inhibits postsynaptic GABA(B) receptors: a mechanism for homeostatic regulation of GABA release in perisomatic synapses. *Mol. Cell. Neurosci.* **24**, 271-282
21. Snapyan, M., Lecocq, M., Guevel, L., Arnaud, M. C., Ghochikyan, A. and Sakanyan, V. (2003) Dissecting DNA-protein and protein-protein interactions involved in bacterial transcriptional regulation by a sensitive protein array method combining a near-infrared fluorescence detection. *Proteomics* **3**, 647-657
22. Smith, P. K., Krohn, R. I., Hermanson, G. T., Mallia, A. K., Gartner, F. H., Provenzano, M. D., Fujimoto, E. K., Goeke, N. M., Olson, B. J. and Klenk, D. C. (1985) Measurement of protein using bicinchoninic acid. *Anal. Biochem.* **150**, 76-85
23. Bradford, M. M. (1976) A rapid and sensitive method for the quantitation of microgram

- quantities of protein utilizing the principle of protein-dye binding. *Anal. Biochem.* **72**, 248-254
24. Eloranta, J. J. and Hurst, H. C. (2002) Transcription factor AP-2 interacts with the SUMO-conjugating enzyme UBC9 and is sumoylated in vivo. *J. Biol. Chem.* **277**, 30798-30804
25. Rodbard, D. (1974) Statistical quality control and routine data processing for radioimmunoassays and immunoradiometric assays. *Clin. Chem.* **20**, 1255-1270
26. Phelps, M., Darley, M., Primrose, J. N. and Blaydes, J. P. (2003) p53-independent activation of the hdm2-P2 promoter through multiple transcription factor response elements results in elevated hdm2 expression in estrogen receptor alpha-positive breast cancer cells. *Cancer Res.* **63**, 2616-2623
27. Filardo, E. J., Quinn, J. A., Bland, K. I. and Frackelton, A. R., Jr. (2000) Estrogen-induced activation of Erk-1 and Erk-2 requires the G protein-coupled receptor homolog, GPR30, and occurs via trans-activation of the epidermal growth factor receptor through release of HB-EGF. *Mol. Endocrinol.* **14**, 1649-1660

28. Yang, X., Hao, Y., Ding, Z., Pater, A. and Tang, S. C. (1999) Differential expression of antiapoptotic gene BAG-1 in human breast normal and cancer cell lines and tissues. *Clin. Cancer Res.* **5**, 1816-1822
29. MacBeath, G. (2002) Protein microarrays and proteomics. *Nat. Genet.* **32** Suppl, 526-532
30. Haab, B. B. (2003) Methods and applications of antibody microarrays in cancer research. *Proteomics* **3**, 2116-2122
31. Sakanyan, V. (2004) High-throughput and multiplexed protein array technology: protein-DNA and protein-protein interactions. *J. Chrom. B (in press)*
32. Lesley, S. A. and Burgess, R. R. (1989) Characterization of the Escherichia coli transcription factor sigma 70: localization of a region involved in the interaction with core RNA polymerase. *Biochemistry* **28**, 7728-7734
33. Thompson, N. E., Hager, D. A. and Burgess, R. R. (1992) Isolation and characterization of a polyol-responsive monoclonal antibody useful for gentle purification of Escherichia coli RNA polymerase. *Biochemistry* **31**, 7003-7008

34. Vassylyev, D. G., Sekine, S., Laptenko, O., Lee, J., Vassylyeva, M. N., Borukhov, S. and Yokoyama, S. (2002) Crystal structure of a bacterial RNA polymerase holoenzyme at 2.6 Å resolution. *Nature* **417**, 712-719
35. Calvert, V. S., Tang, Y., Boveia, V., Wulfkühle, J., Schutz-Geschwender, A., Olive, D. M., Liotta, L. A. and Petricoin, E. F. (2004) Development of Multiplexed Protein Profiling and Detection Using Near Infrared Detection of Reverse-Phase Protein Microarrays. *Clin. Proteomics* **1**, 81-90
36. Boshier, J. M., Totty, N. F., Hsuan, J. J., Williams, T. and Hurst, H. C. (1996) A family of AP-2 proteins regulates c-erbB-2 expression in mammary carcinoma. *Oncogene* **13**, 1701-1707
37. Brown, R. E. (2002) HER-2/neu-Positive breast carcinoma: molecular concomitants by proteomic analysis and their therapeutic implications. *Ann. Clin. Lab. Sci.* **32**, 12-21
38. Wu, S. L., Hancock, W. S., Goodrich, G. G. and Kunitake, S. T. (2003) An approach to the proteomic analysis of a breast cancer cell line (SKBR-3). *Proteomics* **3**, 1037-1046

39. Janes, P.W., Daly, R. J., deFazio, A. and Sutherland, R. L. (1994) Activation of the Ras signalling pathway in human breast cancer cells overexpressing erbB-2. *Oncogene* **9**, 3601-3608
40. Filmus, J., Robles, A. I., Shi, W., Wong, M. J., Colombo, L. L. and Conti, C. J. (1994) Induction of cyclin D1 overexpression by activated ras. *Oncogene* **9**, 3627-3633
41. Lee, R. J., Albanese, C., Fu, M., D'Amico, M., Lin, B., Watanabe, G., Haines, G. K. 3rd, Siegel, P. M., Hung, M. C., Yarden, Y., Horowitz, J. M., Muller, W. J. and Pestell, R. G. (2000) Cyclin D1 is required for transformation by activated Neu and is induced through an E2F-dependent signaling pathway. *Mol. Cell. Biol.* **20**, 672-683.
42. Yu, Q., Geng, Y. and Sicinski, P. (2001) Specific protection against breast cancers by cyclin D1 ablation. *Nature* **411**, 1017-1021.
43. Keyomarsi, K. and Pardee, A. B. Redundant cyclin overexpression and gene amplification in breast cancer cells. (1993) *Proc. Natl. Acad. Sci. U.S.A.* **90**, 1112-1116.
44. Keyomarsi, K., Tucker, S. L., Buchholz, T. A., Callister, M., Ding, Y., Hortobagyi, G. N., Bedrosian, I., Knickerbocker, C., Toyofuku, W., Lowe, M., Herliczek, T. W. and

Bacus, S. S. (2002) Cyclin E and survival in patients with breast cancer. *N. Engl. J. Med.*  
**347**,1566-1575.

## FIGURE LEGENDS

**Figure 1. Schematic representation of the model protocol used to evaluate competitive displacement with one-color detection.** (A) 3D structure of the *T. thermophilus* RNA polymerase (PDB ID: 1IW7). Positions of the epitopes in the three RNAP subunits are circled. (B) Displacement experiments were performed with both purified proteins and crude cell extracts of appropriate recombinant *E. coli* strains. Competition by  $\alpha$ RNAP and RNAP was evaluated both using labeled  $\alpha$ RNAP and labeled RNAP (see text).

**Figure 2. Typical displacement curves obtained for bacterial  $\alpha$ RNAP in one-color detection.** Each curve corresponds to a given concentration (from 0.06 to 1 mg/mL) of immobilized anti- $\alpha$ RNAP antibody as indicated. Ratios of labelled : unlabeled proteins are shown at the top of the plot.

**Figure 3. Assessment of the two-color detection method.** Histograms of competitive displacement assessed in a mixture of Alexa Fluor 680 (A) and IRDye 800CW (B) labeled  $\alpha$ RNAP molecules. The same data is also displayed as displacement curves (C). Experiments were carried out using 12 replicates (4 replicates on 3 slides) with an average standard deviation of 8.6%. Representative fluorescence spots are shown for each ratio.

**Figure 4. Competition between  $\alpha$ RNAP and whole RNAP or between whole RNAP molecules.**

Displacement between labeled lysate of 1 h induced *E. coli* BL21Star (DE3) (pET rpoA-his) and unlabeled purified RNAP (A), labeled lysate of 1 h induced *E. coli* BL21Star (DE3) (pET duet1 his-rpoA, rpoB / pACYC duet1 rpoC, rpoZ) and unlabeled purified  $\alpha$ RNAP (B) or unlabeled purified RNAP (C).

**Figure 5. Expression of RNAP subunits in recombinant *E. coli*.** Western blot of RNAP  $\alpha$ ,  $\beta$  and  $\beta$

subunits synthesized in non-induced (0 h) and IPTG-induced (1-5 h) *E. coli* BL21Star (DE3) (pET duet1 rpoA, rpoB / pACYC duet1 rpoC, rpoZ) strain.

**Figure 6. Comparison of RNAP profiling in bacterial lysates with one-color and two-color**

**fluorescence detection.** (A) One color detection. Displacement of labeled lysates of 1 h induced by unlabeled 1 h induced (1 h\* : 1 h) or by unlabeled 2 h induced (1 h\* : 2 h) lysates of *E. coli* BL21Star (DE3) (pET rpoA-his) cells, and 2 h induced by unlabeled 2 h induced (2 h\* : 2 h) or by unlabeled 1 h induced (2 h\* : 1 h) lysates of *E. coli* BL21Star (DE3) (pET rpoA-his) cells. (B) Competition between two fluorescence dye labeled lysates of 1 h and 5 h induced *E. coli* BL21Star (DE3) (pET duet1 rpoA, rpoB / pACYC duet1 rpoC, rpoZ) strains was assessed with anti- $\alpha$ RNAP, anti- $\beta$ RNAP and anti- $\beta$ RNAP mAbs.

**Figure 7. Protein profiling in breast tumor-derived lines by one-color detection.** Slide 1:

reference array incubated with MDA MB-231 lysate alone labeled with IRDye 800CW; Slide 2: labeled MDA MB-231 lysate mixed at a 1:1 ratio with unlabeled MDA MB-231 lysate; Slide 3: labeled MDA MB-231 lysate mixed at a 1:1 ratio with unlabeled SKBR3 lysate. Spots corresponding to antibodies against proteins found to be overexpressed in SKBR3 cells are indicated.

**Figure 8. Two-color protein profiling in cell lysates from breast tumor lines.** Left-hand array: IRDye 800CW (red) labeled MDA MB-231 lysate versus Alexa Fluor 680 (green) labeled SKBR3; Right-hand array: IRDye 800CW labeled SKBR3 lysate versus Alexa Fluor 680 labeled MDA MB-231. Western blots: left lane = lysate from MDA MB-231 cells and right lane = lysate from SKBR3 cells. Circled numbers refer to position in the array of antibodies used in the corresponding western blot; numbers in bold beside Western blot correspond to NMRAT values. Statistical confidences corresponding to each cutoff level are presented in “Experimental procedures”.

**Figure 9. Differential expression of proteins in breast cancer cell lines using nuclear extracts.**

Graph showing a compilation of data from three two-color profiling experiments performed independently. P was calculated for each target protein using ANOVA. 70% and 90% represent the statistical confidence for the proteins with NMRAT values outside the cutoff levels of 0.82-1.18 and 0.71-1.29, respectively.



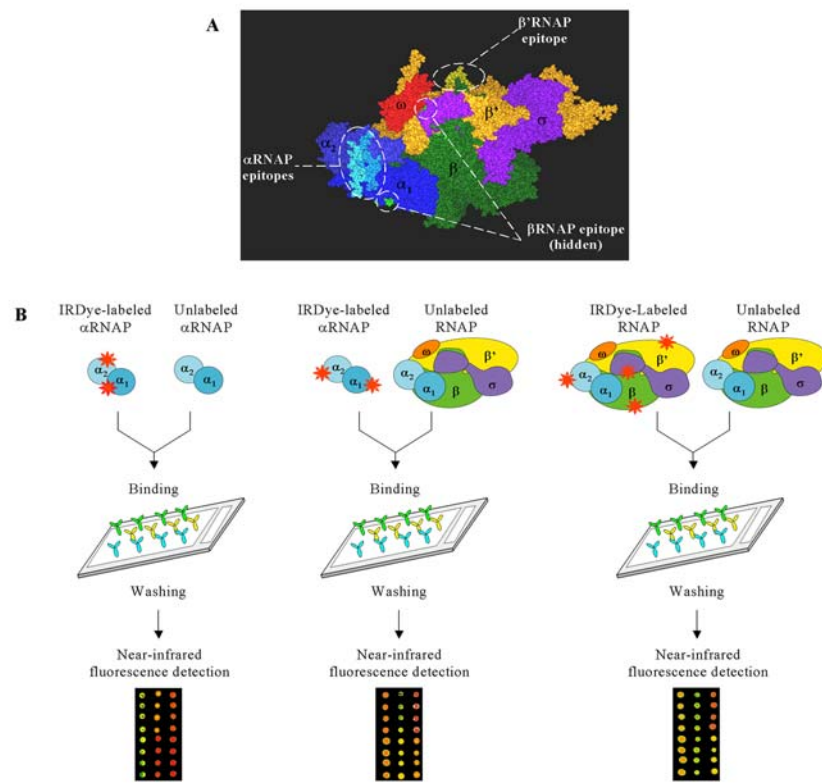


Fig. 1

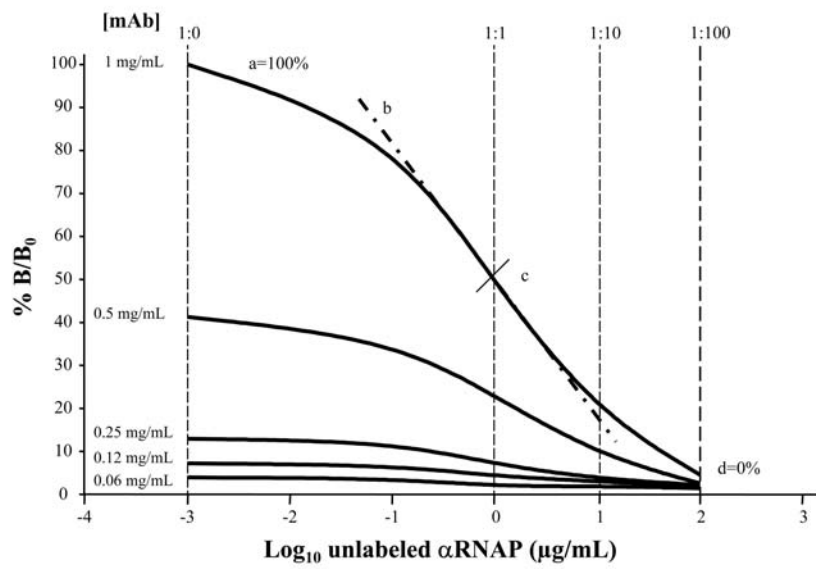


Fig. 2

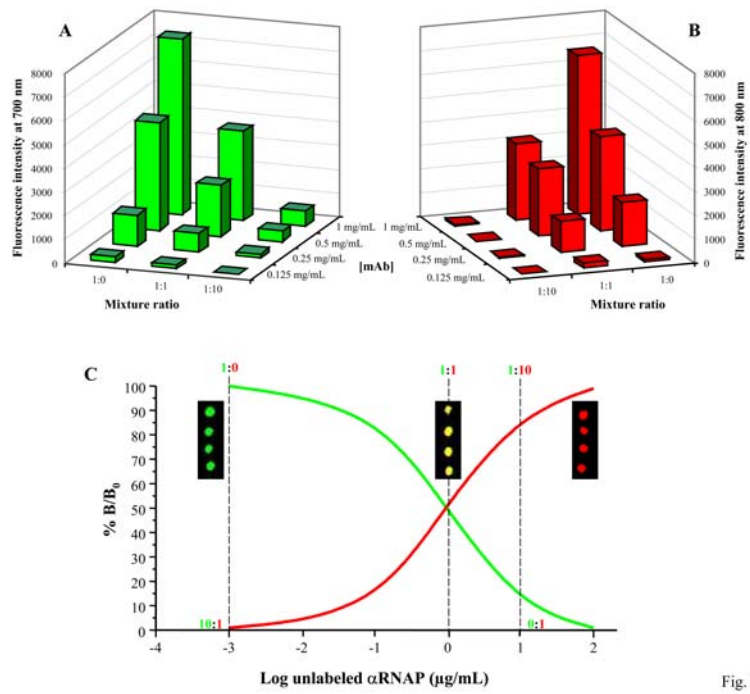


Fig. 3

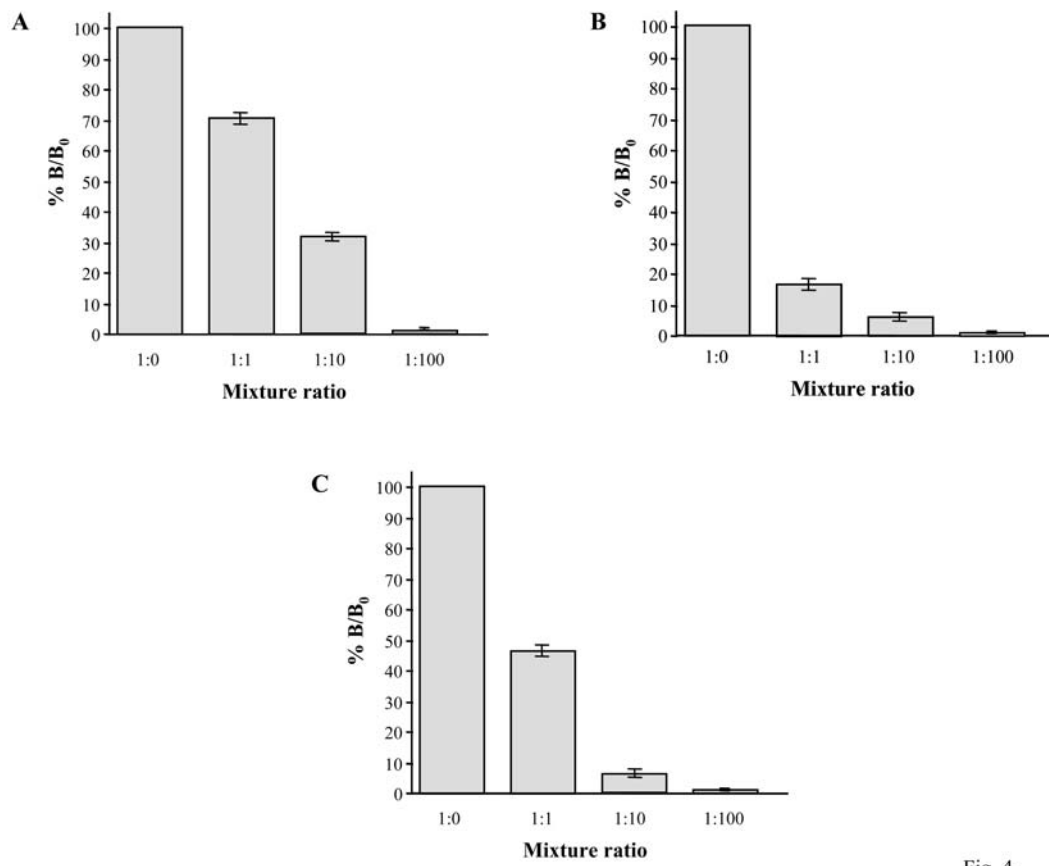


Fig. 4

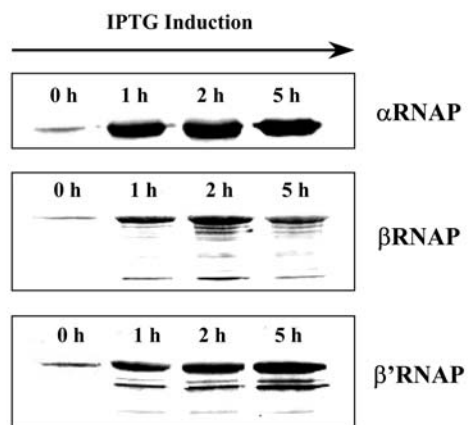


Fig. 5

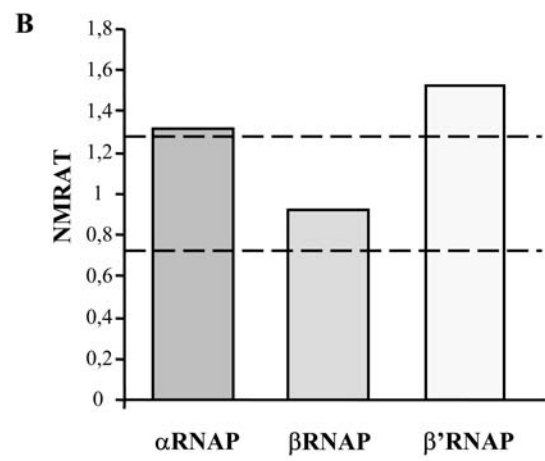
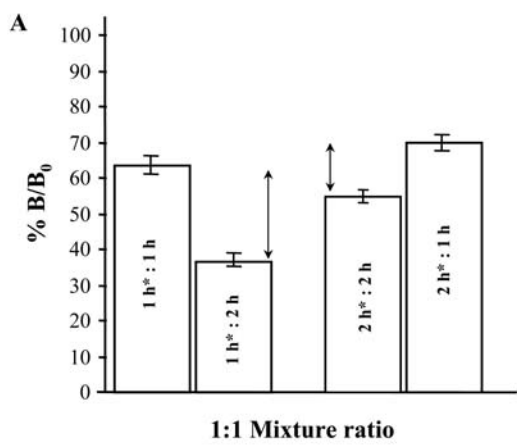


Fig. 6

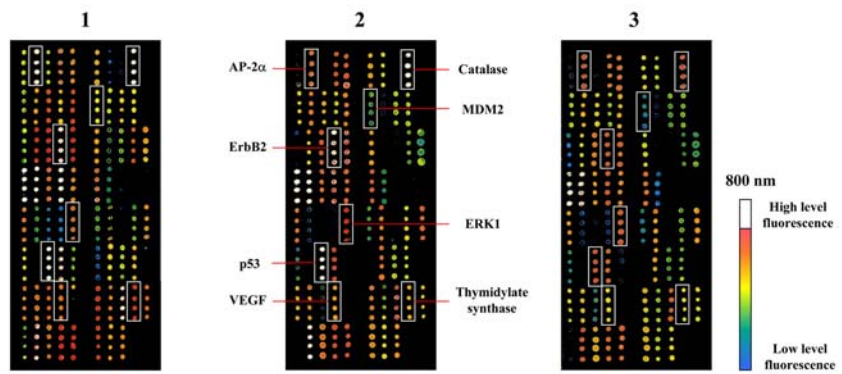
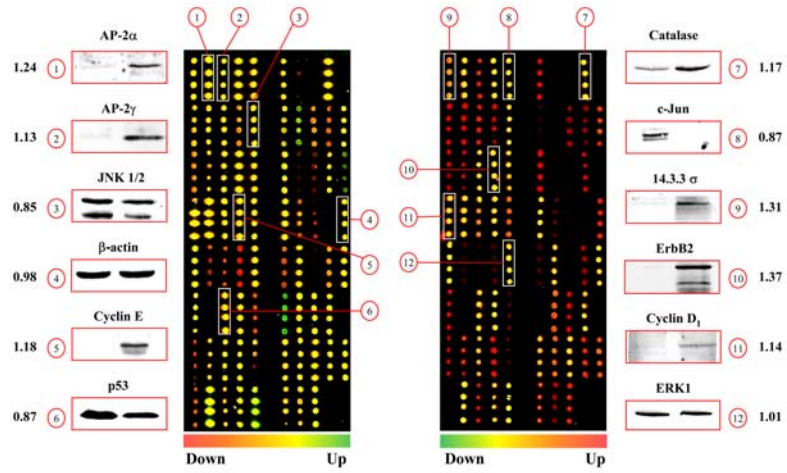


Fig. 7



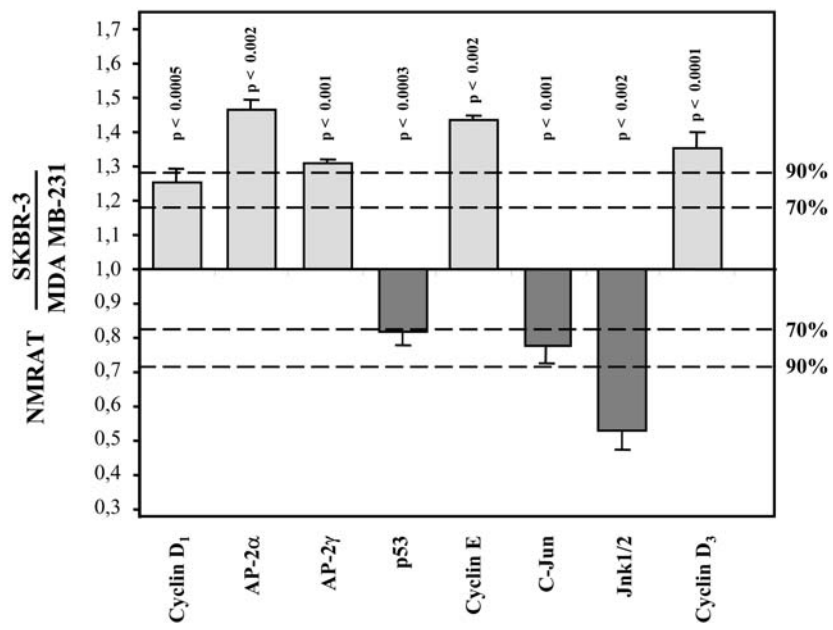


Fig. 9